ORNL/TM-5419

Calculations Pertaining to the Design of a Prebuncher for a 150-MeV Electron Linear Accelerator

R. G. Alsmiller, Jr.
F. S. Alsmiller
J. Barish
T. A. Lewis

OAK RIDGE NATIONAL LABORATORY
OPERATED BY UNION CARBIDE CORPORATION FOR THE ENERGY RESEARCH AND DEVELOPMENT ADMINISTRATION

DISCLAIMER

Printed in the United States of America. Available from
National Technical Information Service
U.S. Department of Commerce
5285 Port Royal Road, Springfield, Virginia 22161
Price: Printed Copy $5.25; Microfiche $3.00

ORNL/TM-5419

Contract No. W-7405-eng-26

Neutron Physics Division

CALCULATIONS PERTAINING TO THE DESIGN OF A PREBUNCHER FOR A 150-MeV ELECTRON LINEAR ACCELERATOR*

R. G. Alsmiller, Jr.
F. S. Alsmiller†
J. Barish‡
T. A. Lewis**

Date Published - October 1977

*Submitted for journal publication.
†Consultant.
‡Computer Sciences Division.
**Instrumentation and Controls Division.

OAK RIDGE NATIONAL LABORATORY
Oak Ridge, Tennessee, 37830
operated by
UNION CARBIDE CORPORATION
for the
DEPARTMENT OF ENERGY

THIS PAGE

WAS INTENTIONALLY

LEFT BLANK

Abstract

Results derived from calculations based on a one-dimensional ballistic model are presented to indicate the extent to which a current pulse of 150-keV electrons containing 1 μC of charge and having a duration of 15 nsec (FWHM) can be bunched by a combination of accelerating and decelerating voltage gaps followed by a drift space. To be useful, the bunched current must be accelerated by an existing accelerator (ORELA), so the calculated results include estimates (upper and lower limits) of the fraction of the bunched beam that will be accelerated. It is found that with 8 voltage gaps the 15-nsec (FWHM) pulse can be reduced to a pulse of $\sim$ 4 nsec (FWHM) in a length $\sim$ 400 cm and that $\sim$ 50% of this bunched pulse will be accelerated by ORELA. The fraction of the bunched pulse that will be accelerated is approximately the same as that for an unbunched pulse.

THIS PAGE

WAS INTENTIONALLY

LEFT BLANK

Acknowledgment

Thanks are due to R. W. Peelle and F. C. Maienschein of the Oak Ridge National Laboratory for many helpful discussions and suggestions throughout the course of this work.

THIS PAGE

WAS INTENTIONALLY

LEFT BLANK

TABLE OF CONTENTS

1. INTRODUCTION

The Oak Ridge Electron Linear Accelerator (ORELA) was designed to produce intense short neutron pulses for the measurement of neutron cross sections by time-of-flight techniques.[1,2] The number of neutrons in an ORELA burst is determined by the total energy of the electrons incident on the target, and thus the suitability of the machine for neutron time-of-flight measurements would be improved if the electron energy in a pulse of given duration could be substantially increased. It is proposed to accomplish this by "prebunching" the electron beam before it enters the accelerator, that is, it is proposed to reduce the pulse without substantially changing the charge in the pulse by passing the beam through a combination of voltage gaps and drift spaces before it enters the accelerator. In this paper, calculated results are presented of the degree of bunching that can be achieved with various combinations of voltage gaps and drift spaces.

In obtaining the results presented here, only the longitudinal motion of the electrons has been considered in detail. The radial motion of the electrons is neglected and the rotational motion of the electrons, due to the presence of a longitudinal magnetic confining field, is included only approximately. Because of the very high charge densities considered here, space-charge effects are large and are taken into account in the calculations. Since the "bunched" electron beam is useful only insofar as it will be accelerated by the existing accelerator, the results presented here include calculated estimates of the fraction of the bunched electron beam that will be accelerated by ORELA.[1,2]

In Section 2 the calculational models are developed and discussed. In Section 3 the results are presented and discussed.

2. CALCULATIONAL PROCEDURE

2.1 Geometric Configuration and Physical Data

In Fig. 1 a schematic diagram of the geometric configuration is shown. The prebuncher is basically a conduction cylinder of radius a (= 2.5 cm) with a series of gaps across which a time-dependent voltage is applied in such a manner that an electron experiences a change in energy as it crosses a gap. In the work reported here, the radius of the electron beam is assumed to be a constant, r_0, throughout the motion. That is, no radial motion is considered, but the rotational motion of the electrons due to the presence of the inhomogeneous (see below) magnetic field is taken into account approximately.

For convenience it is assumed in the calculations that the change in energy of an electron at a gap is instantaneous so that the finite transit time of an electron through a gap may be neglected. The potential differences as a function of time at a gap that can be achieved experimentally and that are used in the calculations is shown in Fig. 2. Two different potential difference curves labeled "decelerating gap" and "accelerating gap" are shown. At a particular gap, i, one or the other of these potential difference curves apply depending on whether the gap is designated as decelerating or accelerating. The time, t_i, is the time when the first electron in a pulse crosses a gap, i.e., in all of the calculations it is assumed that the voltage transient at a gap is timed relative to the time when the first electron in the pulse crosses the gap. Basically, a

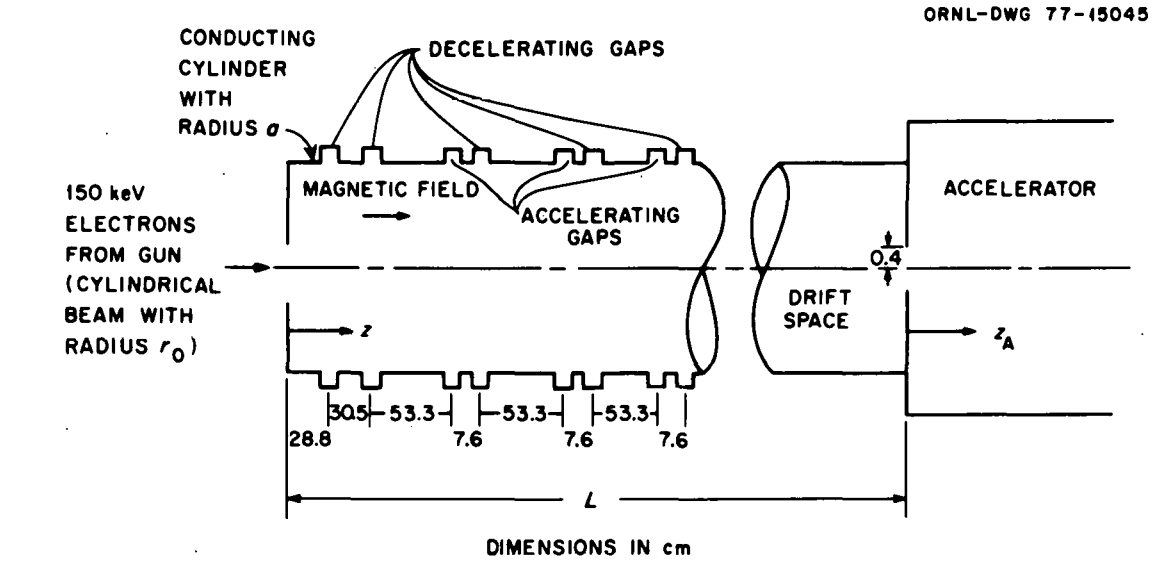

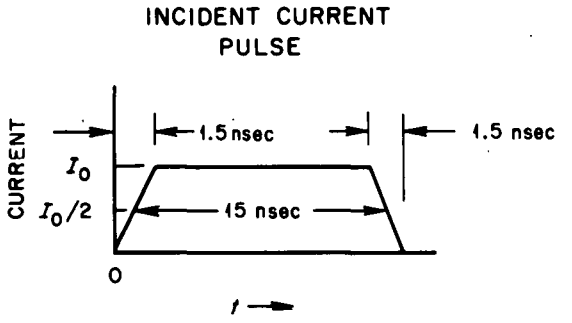

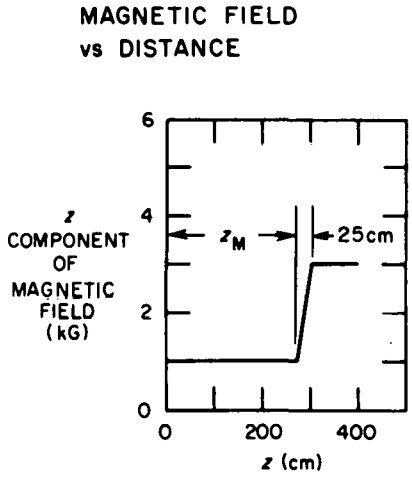

Fig. 1. Schematic diagram of prebuncher geometry. The shape of the incident current pulse is shown in the lower left and the z component of the magnetic field is shown as a function of distance at the lower right.

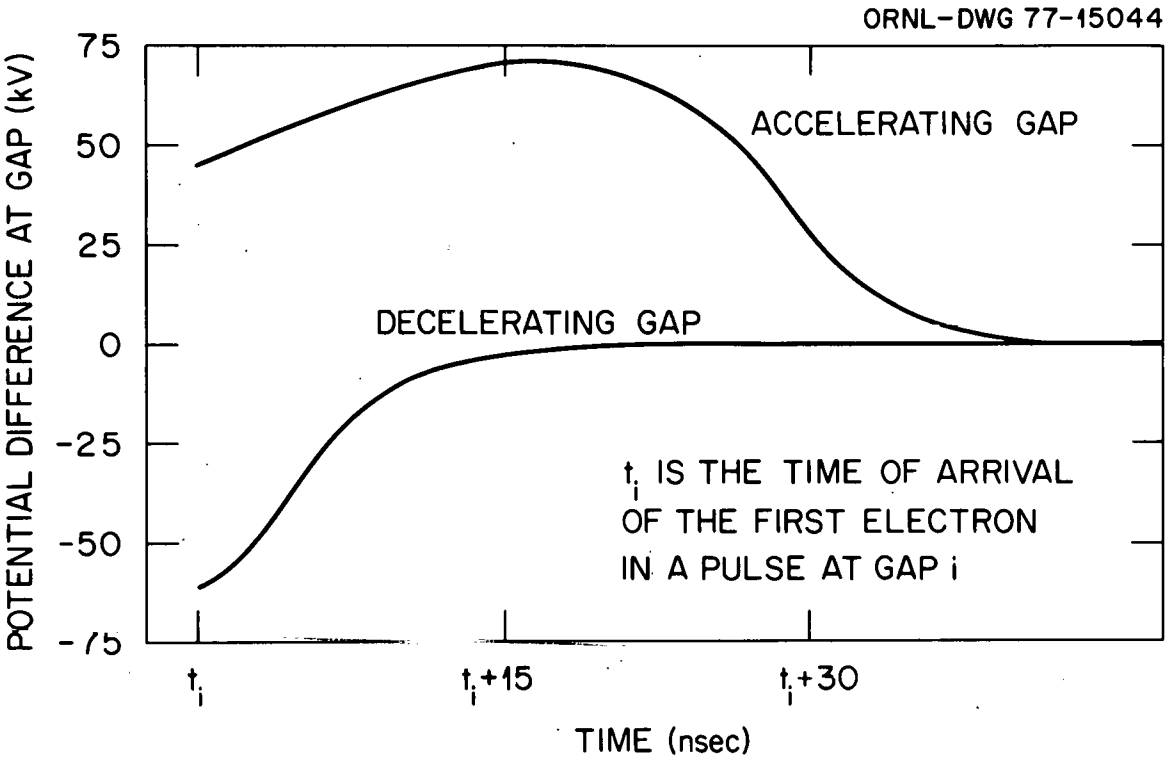

Fig. 2. Potential difference *vs* time at the voltage gaps.

decelerating gap, while slowing down all of the electrons in a pulse, reduces the kinetic energy of the electrons in the front of the pulse relative to the kinetic energy of those in the back of the pulse. An accelerating gap, while accelerating all of the electrons in a pulse, increases the kinetic energy of the electrons in the back of the pulse relative to those in the front of the pulse. It would, of course, be more efficient if deceleration and acceleration could be accomplished at a single gap, but experimentally this has not been possible. The combination of accelerating and decelerating gaps, eight gaps in all, shown in Fig. 1, is the case that is of most interest here, but calculations for other cases will also be shown. The distances between gaps shown in Fig. 8 are determined by the physical dimensions of the gap structure. Any combination of accelerating and decelerating gaps is, in principle, possible, but in practice good "bunching" is obtained only if the electrons in the front of the pulse do not attain negative velocities and this limits the number and positions of decelerating gaps than can be used.

Because space charge effects are large there must be a longitudinal magnetic field to prevent the beam from spreading radially. In the vicinity of the gaps, however, the magnitude of the longitudinal magnetic field that can be produced experimentally is very limited. In the work reported here, a magnetic field of 1 kilogauss is used in the vicinity of the gaps, and this field is increased to 3 kilogauss in the drift space. The longitudinal field that is used is shown in the lower right of Fig. 1. The assumption of a linear increase in the field over a distance of 25 cm is thought to be realistic but is otherwise somewhat arbitrary.

The shape of the current pulse used in the calculations is shown in the lower left of Fig. 1. A linear "rise" and "fall" time of 1.5 nsec is used. This linear assumption and the value 1.5 nsec are somewhat arbitrary, but do not have any appreciable effect on the results. The width of the incident current pulse at half maximum is taken to be 15 nsec so the total duration of the incident pulse is 16.5 nsec. The current, I_0, is determined so that the total charge in the pulse is 1 μC. All electrons are assumed to enter the prebuncher with a kinetic energy, T_0, of 150 keV.

2.2 Trajectory and Current Calculations

The calculations reported here are based on a one-dimensional ballistic model such as that developed by Tien *et al.*,[3] and used by Williams and McGregor[4] and by Tallerico[5] as well as many other investigators.* The starting point of the model is the use of the superposition theorem to express the electric field at a given position and time from the current pulse as a function of parameters describing the current pulse. This is done by means of the equation

$$E(z,t) = \int_0^{t'} dt_0 \; I_0(t_0) E_S[z, z_S(t,t_0), \beta_S(t,t_0)] \quad , \tag{1}$$

where

$$\begin{aligned} t' &= t \qquad \text{if } t < t_{0M} \\ &= t_{0M} \qquad \text{if } t \geq t_{0M} \end{aligned} \tag{2}$$

*A detailed discussion of the ballistic model and references to the extensive literature on this subject has been given by Rowe[6].

and

$E(z,t)$ = the electric field at position z and time t due to the current pulse in the prebuncher,

$I_0(t_0)$ = the current that leaves the electron gun and enters the prebuncher, at time t_0,

t_{0M} = the total time required for the current pulse to enter the prebuncher (= 16.5 nsec). (Note that the zero of time is taken to be the time when the first particle enters the prebuncher.),

$z_S(t,t_0)$ = the position at time t of the charge that entered the prebuncher at time t_0,

$\beta_S(t,t_0)$ = the velocity at time t, divided by the velocity of light, of the charge that entered the prebuncher at time t_0,

$E_S[z,z_S(t,t_0), \beta_S(t,t_0)]$

= the electric field at position z and time t per unit source charge at the position z_S with velocity β_S.

It is assumed in the model that the integral in Eq. (1) may be approximated by a finite sum. If N is an integer that specifies the number of intervals used in approximating the integral in Eq. (1) then

$$E(z,t) \simeq \sum_{j=1}^{N'} Q_j E_S[z,z_j,\beta_j], \tag{3}$$

where

$$\Delta t_0 = \frac{t_{0M}}{N} \tag{4}$$

$$N' = \text{Integer value of } \frac{t}{\Delta t_0} \qquad t < t_{0M}$$
$$= N \qquad t \geq t_{0M} \tag{5}$$

$$\left.\begin{aligned} t_{0j} &= j\Delta t_0 - \frac{\Delta t_0}{2} \\ Q_j &= \int_{t_{0j}-\frac{\Delta t_0}{2}}^{t_{0j}+\frac{\Delta t_0}{2}} dt_0 I_0(t_0) \\ z_j &= z_S(t,t_{0j}) \\ \beta_j &= \beta_S(t,t_{0j}) \end{aligned}\right\} \qquad j = 1, N \tag{6}$$

The equations of motion of the charge Q_i are determined from the relativistic equations of motion of an electron in the electric field, $E(z,t)$, given by Eq. (3), the time-dependent voltage discussed in Section 2.1 and the magnetic field discussed in Section 2.1.

It is assumed throughout this work that there is no radial motion so only the longitudinal and azimuthal equations are of interest. For an electron these equations may be written as

$$\frac{1}{c}\frac{dp_z}{dt} = eE(z,t) + e\sum_{k=1}^{N_G} V_k(t)\delta(z_{Gk}-z) - \frac{e}{c} r \frac{d\phi}{dt} H_r(r,z) \tag{7}$$

$$\frac{d}{dt}\left[\frac{m\gamma r^2}{c^2}\frac{d\phi}{dt} + \frac{e}{c} rA_\phi(r,z)\right] = 0 \tag{8}$$

$$p_z = m\gamma\beta_z \tag{9}$$

$$\gamma = \frac{1}{\sqrt{1-\beta_z^2-\beta_\phi^2}} \tag{10}$$

$$\beta_z = \frac{1}{c}\frac{dz}{dt} \tag{11}$$

$$\beta_\phi = \frac{1}{c}\, r\, \frac{d\phi}{dt} \quad , \tag{12}$$

where

z,r,ϕ = the polar coordinates of the electron,

c = the velocity of light,

p_z = the momentum of the electron multiplied by the velocity of light,

e = the electronic charge,

N_G = the number of voltage gaps,

$V_k(t)$ = the time-dependent voltage on the kth voltage gap,

z_{Gk} = the position coordinate of the kth voltage gap,

$H_r(r,z)$ = the radial component of the magnetic field,

m = the rest energy of the electron,

$A_{\phi(r,z)}$ = the azimuthal component of the magnetic vector potential, i.e., $\vec{H} = \text{curl}\ \vec{A}$,

and in writing Eq. (7) the approximation of infinitesimally thin gaps has been made; i.e., the finite transit time of the electron across the gap has been neglected. If the magnetic field has only an r and z component and if

$$\frac{\partial^2 H_z(z)}{\partial z^2} = 0 \quad , \tag{13}$$

where

$H_z(z)$ = the z component of the magnetic field,

the $A_\phi(r,z)$ may be written as[8]

$$A_\phi(r,z) = \frac{r}{2} H_z(z) \quad , \tag{14}$$

and since

$$H_r(r,z) = - \frac{\partial A_\phi(r,z)}{\partial z} \quad , \tag{15}$$

one has

$$H_r(r,z) = - \frac{r}{2} \frac{\partial H_z(z)}{\partial z} \quad . \tag{16}$$

It will be assumed that the electrons are emitted from the cathode of the electron gun with $\frac{d\phi}{dt} = 0$ and that the cathode is shielded from the magnetic field so the constant of integration in Eq. (8) may be taken to be zero and thus one has

$$\frac{1}{c} \frac{d\phi}{dt} = - e \left(\frac{\mathrm{II}_z(z)}{2m\gamma} \right) . \tag{17}$$

Combining Eqs. (16) and (17) with Eq. (7) gives

$$\frac{1}{c} \frac{dp_z}{dt} = eE(z,t) + e \sum_{k=1}^{N_G} V_k(t) \delta(z_{Gk} - z) - e^2 \left(\frac{r^2}{4m\gamma} \right) H_z(z) \frac{\partial H_z(z)}{\partial z} \quad , \tag{18}$$

where

$$\gamma = \frac{1}{\sqrt{1 - \beta_z^2 - \left[e \frac{r H_z(z)}{2m\gamma} \right]^2}} \quad . \tag{19}$$

Equation (19) is the equation of motion of a single electron. To find the equation of motion of the charge Q_i, Eq. (19) must be averaged over the spatial distribution of charge within Q_i. The basic assumption of the ballistic model as used here is that as a result of this averaging process z in Eq. (19) is evaluated at z_i defined in Eq. (6) and r^2 in Eq. (19) is evaluated at the mean value $\frac{r_o^2}{2}$ where r_o is the radius of the beam. With this ansatz the equation of motion of the charge Q_i becomes

$$\frac{1}{c}\frac{dp_i}{dt} = Q_i \sum_{\substack{j=1 \\ j\neq i}}^{N'} Q_j E_s(z_i, z_j, \beta_j)$$

$$+ Q_i \sum_{k=1}^{N_G} V_k(t)\delta(z_{Gk} - z_i)$$

$$- Q_i \, e \left[\frac{r_o^2}{8m\gamma}\right] H_z(z_i) \frac{\partial H_z(z_i)}{\partial z_i} \qquad (i = 1 \text{ to } N) \qquad (20)$$

$$p_i = M_i \gamma_i \beta_i \qquad (21)$$

$$\beta_i = \frac{1}{c}\frac{dz_i}{dt} \qquad (22)$$

$$\gamma_i = \frac{1}{\sqrt{1-\beta_i^2 - \left[\frac{e r_o H_z(z_i)}{2\sqrt{2}\, m\gamma_i}\right]^2}} \, , \qquad (23)$$

where

M_i = the rest energy of the charge Q_i.

The term i = j in the first sum on the right of Eq. (20) has been omitted since it is assumed that the charge Q_i does not exert a force on itself. Equation (20) is taken to be valid for all i from 1 to N. This set of equations then forms a complete set for the determination of $z_i(t)$ and $\beta_i(t)$ for all i. In the approximation used here the equation of motion of the charge Q_i is essentially the equation of motion of a single electron, i.e., the basic ansatz of the model is that the motion of the charge Q_i may be identified with the motion of an electron. The presence of the magnetic confining field is included only approximately in Eq. (20), but the approximation does allow for the fact that as an electron enters the higher magnetic field it acquires additional rotational energy and this energy must be removed from its longitudinal motion. It should be noted that the approximation used determines only the central position (in z) of Q_i and not the distribution in space of the charge Q_i. The assumption that is made to calculate the current at a particular position as a function of time when only this central position is known is discussed below.

Before the set of equations given by Eq. (20) can be solved numerically, it is necessary to specify the form of E_S. The form used in the work

reported here is essentially that derived by Williams and McGregor[4*] and is

$$E_S(z_i,z_j,\beta_j) = \frac{2}{r_0^2} \sum_{r=i}^{\infty} \exp(-\gamma_{zj}\frac{\gamma_r}{a}|z_i-z_j|) \left[\frac{2J_1\left(\gamma_r\frac{r_0}{a}\right)}{\gamma_r J_1(\gamma_r)}\right]^2 \text{sign}(z_i-z_j) \quad (24)$$

$$\gamma_{zj} = \frac{1}{\sqrt{1-\beta_j^2}} , \quad (25)$$

---

*Williams and McGregor[4] apparently used for the exponential in Eq. (24),

$$\exp[-\tfrac{1}{2}(\gamma_{zi}+\gamma_{zj})\frac{\gamma_r}{a}|z_i-z_j|] ,$$

rather than the expression

$$\exp(-\gamma_{zj}\frac{\gamma_r}{a}|z_i-z_j|) ,$$

which is used here. Both forms are, of course, very approximate. The derivation of the form used here is given in Appendix I.

where

r_0 = the radius of the beam;

a = the radius of the conducting cylinder;

J_α = a Bessel function of the first kind,[7]

γ_r = the $r^{\underline{th}}$ root of J_0.

With the boundary conditions specified previously, i.e., that for all i the electron at the center of Q_i enters the prebuncher ($z = 0$) at the time t_{0i}, Eqs. (20)-(23) may be solved to give

$$z = z(t,t_0) \tag{26}$$

$$z_i = z(t,t_{0i}) \quad i = 1 \text{ to } N' , \tag{27}$$

or, provided that the center of particle i actually reaches the depth z, Eqs. (20)-(23) may be solved to give

$$t = t(z,t_0) \tag{28}$$

$$t_i = t(z,t_{0i}), \tag{29}$$

where

t_i = the time when the electron at the center of Q_i, that enters the prebuncher at time t_{0i}, is at position z.

There is nothing in the model to prevent negative velocities and thus it is possible, and sometimes happens, that the center of charge Q_i does not reach a depth z, in which case Eq. (29) does not yield a real value for t_i. In the trajectory calculation this possibility causes no difficulty, but it

does necessitate special consideration when the current as a function of time at a depth z is considered.

To calculate the current as a function of time at a particular point z due to all charge, let us first consider the current due to a small element of charge. By conservation of charge one has

$$I'(z,t)dt = I_o(t_o)dt_o \quad , \tag{30}$$

where

$I'(z,t)$ - the current at z at time t due to the current that entered the prebuncher at time t_o.

If the right side of Eq. (30) is integrated over the interval t_{oj} to $t_{o,j+1}$, if $I'(z,t)$ is assumed to be constant during this integration, and if the centers of the charges Q_j and Q_{j+1} reach the depth z, then

$$I_j(z,t) = F(t,t_j,t_{j+1}) \times \left[\frac{\int_{t_{oj}}^{t_{o,j+1}} I_o(t_o)dt_o}{|t_{j+1}-t_j|} \right] \qquad \begin{array}{l}\text{(if the centers of } Q_j \text{ and } Q_{j+1} \\ \text{reach the depth z)}\end{array} \tag{31}$$

$$F(t,t_j,t_{j+1}) = [\Theta(t_{j+1}-t)\Theta(t-t_j)\Theta(t_{j+1}-t_j) + \Theta(t_j-t)\Theta(t-t_{j+1})\Theta(t_j-t_{j+1})] \tag{32}$$

$$\begin{aligned} \Theta(x) &= 1 \quad x > 0 \\ &= 0 \quad x < 0 \quad , \end{aligned} \tag{33}$$

where

$I_j(z,t)$ = the current at z at time t due to the charge that enters the prebuncher in the time interval t_{oj} to $t_{o,j+1}$,

and since

$$\int_{t_{oj}}^{t_{o,j+1}} I_o(t_o)dt_o = \frac{1}{2}(Q_j + Q_{j+1}) \tag{34}$$

$$I_j(z,t) = F(t,t_j,t_{j+1}) \frac{\frac{1}{2}(Q_j+Q_{j+1})}{|t_{j+1}-t_j|} . \tag{35}$$

The absolute value in Eq. (31) must be introduced since particles may pass during the motion and thus there is no assurance that $t_{j+1} > t_j$. It should be noted that in writing Eq. (31) the drastic assumption has been made that even when particles pass during the motion; i.e., when $t_{j+1} < t_j$, the charge that entered the prebuncher in the time interval t_{oj} to $t_{o,j+1}$ crosses the plane at z in the time interval $|t_{j+1}-t_j|$. If the center of charge Q_{j+1} does not reach the depth z then it is assumed that

$$I_{j+1}(z,t) = 0 \qquad \text{(if center of } Q_{j+1} \text{ does not reach depth z)} \tag{36}$$

and the current $I_j(z,t)$ is defined by

$$I_j(z,t) = F(t,t_j,t_{j+2}) \frac{\frac{1}{2}[Q_j+Q_{j+2}]}{|t_{j+2}-t_j|} \qquad \text{(if centers of } Q_j \text{ and } Q_{j+2} \text{ reach depth z and the center of } Q_{j+1} \text{ does not)} , \tag{37}$$

where $F(t,t_j,t_{j+2})$ is defined by Eq. (32). Equations analogous to Eqs. (34) and (35) are used if the centers of two successive charges, i.e., Q_{j+1} and Q_{j+2}, do not reach the depth z.

With the current $I_j(z,t)$ defined for all j, the total current I(z,t) from all charges including the all important overlap of charge is given by

$$I(z,t) = \sum_{j=1}^{N'-1} I_j(z,t) \quad . \tag{38}$$

For simplicity in writing the current equations, the small amount of charge that enters the prebuncher in the time interval 0 to $\frac{\Delta t_o}{2}$ and 16.5 nsec - $\frac{\Delta t_o}{2}$ to 16.5 nsec has been neglected. There is no difficulty about including this charge and it was included in all calculations.

2.3 Fraction of the Current Pulse That Will Be Accelerated

Only some portion of the current pulse that is incident on the accelerator will actually be accelerated to high energy and emerge from the accelerator. This portion is known to be of the order of 50% at ORELA under present operating conditions with an unbunched beam.[8] However, this fraction is dependent on the energy distribution of the particles in the current pulse, and this energy distribution is very different in the bunched pulse from that in the unbunched pulse, so it is important to have estimates of the fraction of the bunched pulse that will be accelerated. Such estimates have been obtained by using a theory developed by Slater.[8] The theory is described in detail in Ref. 8 so only a brief outline will be given here.

In the Slater theory, only the longitudinal motion of the electrons is considered, and it is assumed that only a single-velocity component, i.e., the "dominant" mode, of the traveling wave in the accelerator need be considered. Furthermore, it is assumed that the electric field strength of this dominant mode in the longitudinal direction is sufficiently large that space-charge effects may be neglected. Under these circumstances, the equations of motion of the $i^{\underline{th}}$ electron to enter the accelerator may be written[8]

$$\frac{dp_{Ai}}{dt} = ecE_{A0} \sin 2\pi\nu(t - t_{A10} - \frac{z_{Ai}}{c} + \phi) \tag{39}$$

$$p_{Ai} = \frac{m \beta_{Ai}}{\sqrt{1-\beta_{Ai}^2}} \tag{40}$$

$$\beta_{Ai} = \frac{1}{c} \frac{dz_{Ai}}{dt} \tag{41}$$

where

p_{Ai} = the longitudinal momentum of the ith electron in the accelerator;

e = the electron charge,

m = the electron rest energy,

E_{A_0} = the amplitude, before any electron acceleration, of the longitudinal electric field for the dominant mode of the traveling wave (= 0.1 MV cm^{-1} in ORELA),

ν = the frequency of the dominant mode of the traveling wave (= 1.3×10^9 sec^{-1} in ORELA),

t_{A10} = the time when the first electron in the current pulse enters the accelerator,

z_{Ai} = the longitudinal coordinate of a particle measured from the entrance to the accelerator,

c = the velocity of light and the velocity of the dominant mode of the traveling wave in ORELA,

ϕ = an arbitrary phase,

and from the equations of motion, it follows that H, defined by

$$H = \sqrt{m^2 + p_{Ai}^2} - p_{Ai} - e E_{A0} \frac{c}{2\pi\nu} \cos 2\pi\nu\left(t - t_{A10} - \frac{z_{Ai}}{c} + \phi\right) , \tag{42}$$

is a constant of the motion. The constant t_{A10} could be absorbed into the arbitrary phase ϕ, but for clarity this has not been done. By analyzing H as a function of the argument of the cosine, Slater shows that there is a minimum incident momentum of an electron $(p_A)_{MIN}$, given by

$$(p_A)_{MIN} = \frac{m^2 - 4(e\, E_{A0}\, \frac{c}{2\pi\nu})^2}{4\, e\, E_{A0}\, \frac{c}{2\pi\nu}} , \tag{43}$$

such that an electron that enters the accelerator with momentum less than this minimum cannot be accelerated to high energy. Furthermore, from H it can be shown that if

$$p_{Ai0} \geq (p_A)_{MIN} , \tag{44}$$

where

p_{Ai0} = the longitudinal momentum of the ith electron at the entrance to the accelerator,

and

$$H_L = \sqrt{m^2 + (p_A)^2_{MIN}} - (p_A)_{MIN} + e\, E_{A0}\, \frac{c}{2\pi\nu} , \tag{45}$$

then those electrons such that

$$\cos 2\pi\nu\, (t_{Ai0} - t_{A10} + \phi) \leq \frac{\sqrt{m^2 + p^2_{Ai0}} - p_{Ai0} - H_L}{e\, E_{A0}\, \frac{c}{2\pi\nu}} , \tag{46}$$

where

t_{Ai0} = the time when the ith electron in the current pulse enters the accelerator,

will be accelerated. The phase of the wave in ORELA when the first particle in the current bunch enters the accelerator is arbitrary. To simulate this in the calculations, the arbitrary phase ϕ is introduced and an average is carried out over all values of ϕ.

The probability, $P_U(L,p_{Ai0},\phi)$ that the ith electron which enters the accelerator will be accelerated to high energy may be written as

$$P_U(L,p_{Ai0},\phi) = 1 \text{ if Eq. (46) is satisfied}$$
$$= 0 \text{ if Eq. (46) is not satisfied,} \qquad (47)$$

where L denotes the entrance to the accelerator (see Fig. 1) and the probability averaged over all phases, $\overline{P}_U(L,p_{Ai0})$, is

$$\overline{P}_U(L,p_{Ai0}) = \frac{1}{2\pi} \int_0^{2\pi} P_U(L,p_{Ai0},\phi)d\phi. \qquad (48)$$

The subscript U means "upper" since the theory presented in this Section gives an upper limit on the current that will be accelerated as explained in Section 2.4. The assumption will be made that $\overline{P}_U(L,p_{Ai0})$ may be applied to a group of electrons, but, even so, the fraction of the current $I_j(L,t)$, given by Eq. (46) that will be accelerated cannot be found by multiplying $I_j(L,t)$ by $\overline{P}_U(L,p_{Ai0})$ because $I_j(L,t)$ contains electrons with a variety of momenta. To overcome this difficulty, let

$$n(j)\Delta t = t_{j+1} - t_j \ , \qquad (49)$$

where n(j) is the smallest integer such that

$$\Delta t_{MIN} \geq \Delta t \qquad (50)$$

and Δt_{MIN} is a time interval which must be specified. Then let

$$t_{jk} = t_j + k\Delta t \qquad k = 0 \text{ to } n(j) \qquad (51)$$

$$I_{jk}(z,t,p_{jk}) = I_j(z,t)\ \Theta[t-t_{j(k-1)}]\ \Theta[t_{jk}-t] \qquad k = 1 \text{ to } n(j), \tag{52}$$

where the momentum p_{jk} associated with the current I_{jk} is found at $t_{jk} - \frac{\Delta t}{2}$ by linear interpolation between $p_j(z)$ and $p_{j+1}(z)$. Then

$$I_U(L,t) = \sum_{j=1}^{N-1} \sum_{K=1}^{n(j)} I_{jK}(L,t,p_{jK})\overline{P}_U(L,p_{jk}) \tag{53}$$

where

$I_U(L,t)$ = the current (upper limit) as a function of time at the entrance to the accelerator that will be accelerated.

In the calculations, the time Δt_{MIN} was taken to be 0.05 nsec. If Eq. (37) rather than Eq. (35) applies then t_{j+2} rather than t_{j+1} is used in Eq. (49).

2.4 Beam Loading

The theory described in Section 2.3 allows a determination of the fraction of the current pulse incident on the accelerator that will be accelerated if the amplitude of the longitudinal electric field for the dominant mode of the traveling wave in the accelerator, E_{A0}, is known. For a constant gradient linear accelerator like ORELA,[1] however, this amplitude is not a constant but varies with the amount of charge that is accelerated, and thus, to calculate the fraction of the incident current pulse that will be accelerated, it is necessary to take into account this variation. The theory of how this amplitude varies under transient conditions has been discussed in detail by Neal[9] and by Leiss,[10] and it is the results of these

authors that will be utilized here. In this section, only a brief discussion is presented, but a detailed derivation of the results used here is given in Appendix 2.

If

$E_A(z_A, t - t_{A10})$ = the amplitude of the longitudinal electric field of the dominant mode of the traveling wave at position z_A and any time t after the first electron in the current pulse enters the accelerator,

it can be shown that for sufficiently large z_A

$$E_A(z_A, t - t_{A10}) = E_{A0} - K i_A[t - t_{A10} - \frac{z_A}{c}] \quad , \tag{54}$$

where

K = a constant,

i_A = the accelerated current (assumed constant in the derivation of Eq. (54)),

c = the particle velocity in the accelerator which is assumed to be approximately the velocity of light.

The equation of motion of the ith electron traveling down the accelerator may be written approximately as

$$z_{Ai} = c(t - t_{Ai0}) \quad , \tag{55}$$

and then $E(z_A,t)$ evaluated at the position of the ith electron becomes

$$E_A(z_{Ai},t) = E_{A0} - Ki_A(t_{Ai0} - t_{A10}) = E_{A0} - K Q_{Ai} \quad , \tag{56}$$

where

Q_{Ai} = the charge that is being accelerated ahead of the ith electron.

Basically, Eq. (54) is applicable only for z_A values such that the current i_A may be assumed to be constant (i.e., particles are no longer being lost from the beam that is being accelerated) and such that the electron velocity is sufficiently relativistic that it may be assumed to be approximately the velocity of light.

The value of K in Eq. (56) was determined from measurements made at ORELA by Pering and Lewis.[1] If the ambiguity in the energy change of the particles at small z_A is neglected, then it follows from Eq. (56) that the energy spread of the beam as it leaves the accelerator, $\Delta\varepsilon$, is given by

$$\Delta\varepsilon = K\, e\, Q_A L_A \ , \tag{57}$$

where

Q_A = the total charge accelerated, and

L_A = the length of the accelerator.

The relation in Eq. (57) has been verified for a range of Q_A values by the measurements in Ref. 1, and from these measurements, the value of K for ORELA was determined to be 7.27 MV $(\mu C)^{-1}$ m^{-1}. This is the value used in obtaining the results with beam loading given in Section 3.

Equation (56) indicates that the amplitude of the electric field at the position of the ith particle as it travels in the accelerator is a constant independent of time. This means that the theory of Section 2.3 could be applied except that Eq. (56) is valid only for large z_{Ai}, and the theory of Section 2.3 must be applied at small z_{Ai}. When Eq. (56) is used at small z_{Ai}, it is not clear what value of Q_{Ai} should be used, but it is clear that a lower limit on the field, and thus the fraction of charge accelerated, will be obtained if Q_{Ai} is put equal to all of the incident charge that has entered the accelerator from t_{A1o} to t_{Aio}, and this is the approximation that is made here.

With $E_A(z_{Ai},t)$ determined from Eq. (56), the probability, $\overline{P}_L(L,p_{Ai_0})$, that the $i^{\underline{th}}$ electron that enters the accelerator will be accelerated may be defined in the same manner as $\overline{P}_U(L,p_{Ai_0})$ with E_{A0} replaced by E_A, and then

$$I_L(L,t) = \sum_{j=1}^{N'-1} \sum_{K=1}^{n(j)} I_{jK}(L,t,p_{jK})\overline{P}_L(L,p_{jk}) \quad , \tag{58}$$

where

$I_L(L,t)$ = the current as a function of time at the entrance to the accelerator that will be accelerated when beam loading in the approximation described above is used.

Since the effects of beam loading have been overestimated, the quantity $I_L(L,t)$ is a lower limit on the current that will be accelerated. On the other hand, $I_U(L,t)$ is obtained by neglecting beam loading and gives, therefore, an upper limit on the current that will be accelerated.

3. RESULTS AND DISCUSSION

Calculated results for several cases of interest in the design of the ORELA prebuncher are given in Figs. 3-6. Each figure corresponds to a particular configuration of decelerating and accelerating voltage gaps and specific values of the magnetic field parameter, z_M, (see Fig. 1). In all cases, the radius of the conducting cylinder, a, is 2.5 cm, and in all cases except that considered in Fig. 6, the radius of the beam, r_o, is 0.4 cm. The total charge in the incident beam was taken to be 1 μC.

The results presented in each figure represent the current as a function of time (at the entrance to the accelerator) that will be accelerated for specific values of the length, L, of the prebuncher. For each L value, the zero of time is taken to be the time when the first electron enters the accelerator. For each L value considered, the current as a function of time is given "without beam loading" and "with maximum beam loading." As explained in Section 2.4, the beam-loading approximation used here gives an overestimate of the effects of beam loading, and thus the current "with maximum beam loading" is a lower limit on the current that will be accelerated. Similarly, the calculated current "without beam loading" is an upper limit on the current that will be accelerated, and thus the two curves for each L value bracket the current, as a function of time, that will be accelerated. Because of the many ⊛ functions which occur in $I_U(L,t)$ and $I_L(L,t)$ given by Eq. (53) and (58) these functions contain many stepwise discontinuities. To avoid these discontinuities, insofar as possible, the functions $I_U(L,t)$ and $I_L(L,t)$ have been averaged over a sequence of small time intervals to produce histograms. It is these histograms that are presented in Figs. 3-6. Also given for each L value in each figure are the total charges that will be accelerated and the second moments of the current distributions defined by

$$Q_\alpha(L) = \int_0^\infty I_\alpha(L,t)dt$$

$$\bar{t}_\alpha(L) = \frac{1}{Q_\alpha(L)} \int_0^\infty I_\alpha(L,t)tdt$$

$$\sigma_\alpha(L) = \left\{ \frac{1}{Q_\alpha(L)} \int_0^\infty I_\alpha(L,t)\,[t-\bar{t}_\alpha(L)]^2 dt \right\}^{1/2}$$

where α takes values U for the case without beam loading and L for the case with maximum beam loading.

In Figs. 3-5, calculated results are given for the case of 7, 8, and 9 voltage gaps, respectively. The results in Fig. 4 were obtained with the decelerating gap-accelerating gap configuration shown in Fig. 1. The voltage gap configuration used in obtaining the results in Fig. 3 is the same as that shown in Fig. 1 except that the last decelerating gap before the drift space was removed. The voltage gap configuration used in obtaining the results in Fig. 5 is the same as that shown in Fig. 1 except that an additional decelerating gap has been added at 30.48 cm after the last gap shown. In obtaining all of the results in Figs. 3-5 the decelerating gap-accelerating gap configuration for the first seven gaps is the same. The actual configuration of these seven gaps is somewhat arbitrary, but not entirely so since, as a general rule, it seems undesirable that the particles in front of the pulse attain a negative velocity.

In obtaining Fig. 3, the magnetic field parameter z_M (see Fig. 1) was taken to be 250 cm, and in obtaining Figs. 4 and 5, z_M = 275 and 300 cm, respectively. In all cases, the value of z_M was chosen to be near the beginning of the drift space. As stated previously, the magnitude of the magnetic field that can be produced in the vicinity of the gaps is limited, and, therefore, the assumption is made that to prevent the radial spreading of the beam it is desirable to increase the magnetic field strength to its final value near the beginning of the drift space.

The curves at the top of Fig. 3 are for L = 0.0 cm and thus correspond to the case when the current pulse enters the accelerator directly

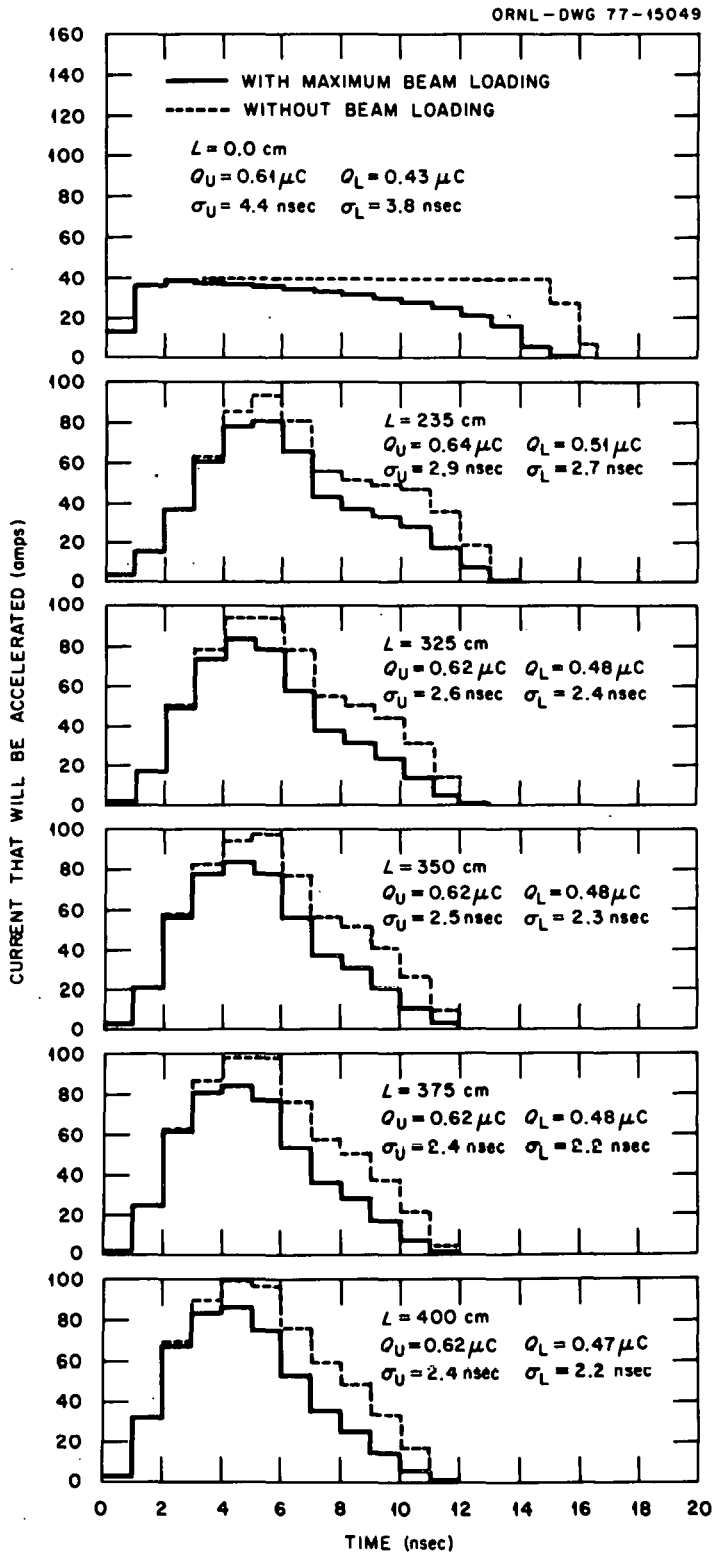

Fig. 3. Current that will be accelerated *vs* time for a 7-voltage gap configuration. (The dashed histogram is the upper bound and the solid histogram is the lower bound) (Q = 1 μC, r_o = 0.4 cm).

from the electron gun. The decrease with increasing time of the solid curve for L = 0.0 cm is due to beam loading (i.e., the electric field strength decreases as particles are accelerated and thus the particles that enter the accelerator at the later time find a much reduced field strength and have a correspondingly lower probability of being accelerated). The total charge that will be accelerated without beam loading, Q_U, equals .61 μC and the total charge that will be accelerated with maximum beam loading, Q_L, equals .43 μC. ORELA operating experience indicates that approximately 0.5 μC of a 1 μC pulse will be accelerated, thus confirming that Q_U and Q_L as calculated here are upper and lower limits on the current that will be accelerated.

The other sets of histograms in Fig. 3 correspond to increasingly larger values of L. The second set of histograms from the top of the figure (L = 235 cm) show the result when there is no drift space, that is, the current pulse enters the accelerator immediately after passing through the last voltage gap. At L = 325 cm a modest amount of bunching has occurred and the amount of bunching - as indicated by σ_U and σ_L - increases slowly as L increases to 400 cm. At all L $\geq$ 235 cm the upper and lower limits on the current distributions are similar in shape. It should be noted that Q_U and Q_L for all L values considered are not significantly different so that the total charge that will be accelerated has not been appreciably affected by the bunching process. The largest L value considered (= 400 cm) was primarily dictated by the available space at ORELA[3], but because of radial confinement problems that are not considered here, it seems desirable to keep the total length of the prebuncher as short as possible.

To obtain more bunching than that shown in Fig. 3, a larger velocity gradient across the current pulse is needed so in Fig. 4 results are shown for an 8-gap configuration (see Fig. 1). The various sets of histograms in Fig. 4 correspond to different L values as indicated. The histograms for L = 0.0 cm are not shown since they are the same as those shown in Fig. 3. The histograms at L = 242 cm again correspond to the case when the particles enter the accelerator immediately after leaving the last voltage gap. At L = 325 cm the bunching in Fig. 4 is somewhat better than the bunching in Fig. 3 and this continues to be the case at the larger L values. The total current that will be accelerated is very approximately the same at all L values in both Figs. 3 and 4. In Fig. 4, the best bunching is achieved at L = 400 cm, but the degree of bunching is changing only slowly with distance so the exact length of the prebuncher is not of critical importance.

In Fig. 5 results are given for the 9-voltage gap configuration; i.e., for one decelerating gap in addition to those used in obtaining the results in Fig. 4. The set of histograms at the top of the figure (L=273) correspond to the case when the particles enter the accelerator immediately after leaving the last voltage gap. The most striking feature of the results for L $\geq$ 325 cm in Fig. 5 compared to those in Figs. 3 and 4 is the appearance of a "tail" on the current distribution calculated without beam loading. This "tail" corresponds to particles that lag behind the main pulse. In Fig. 5, the "tails" are shown only out to 20 nsec, but they do extend beyond this time. Tails similar to those shown in Fig. 5 also occur in Figs. 3 and 4, but the magnitude of the current in the tail

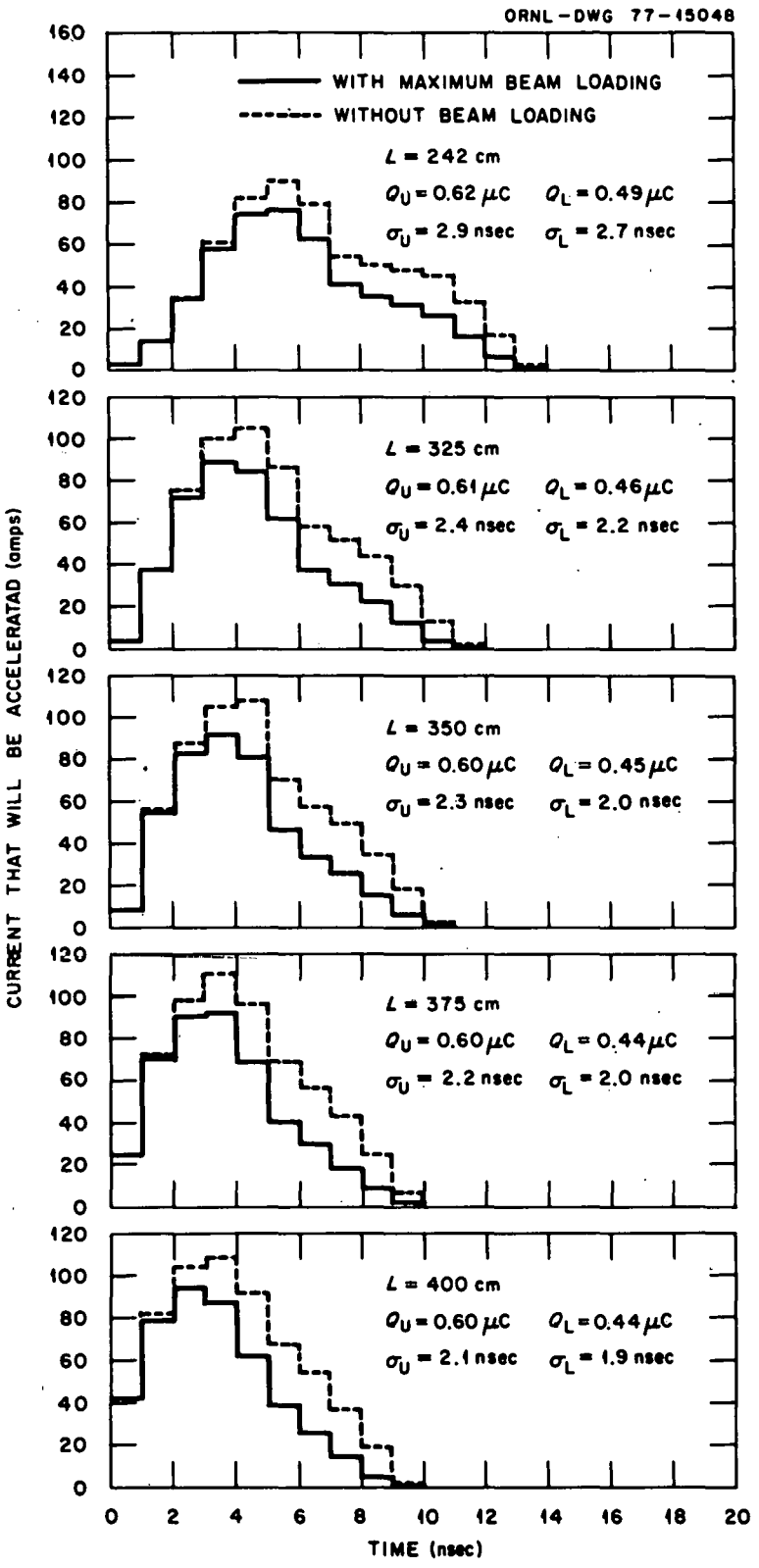

Fig. 4. Current that will be accelerated *vs* time for an 8-voltage gap configuration. (The dashed histogram is the upper bound and the solid histogram is the lower bound.) (Q = 1 μC, r_o = 0.4 cm).

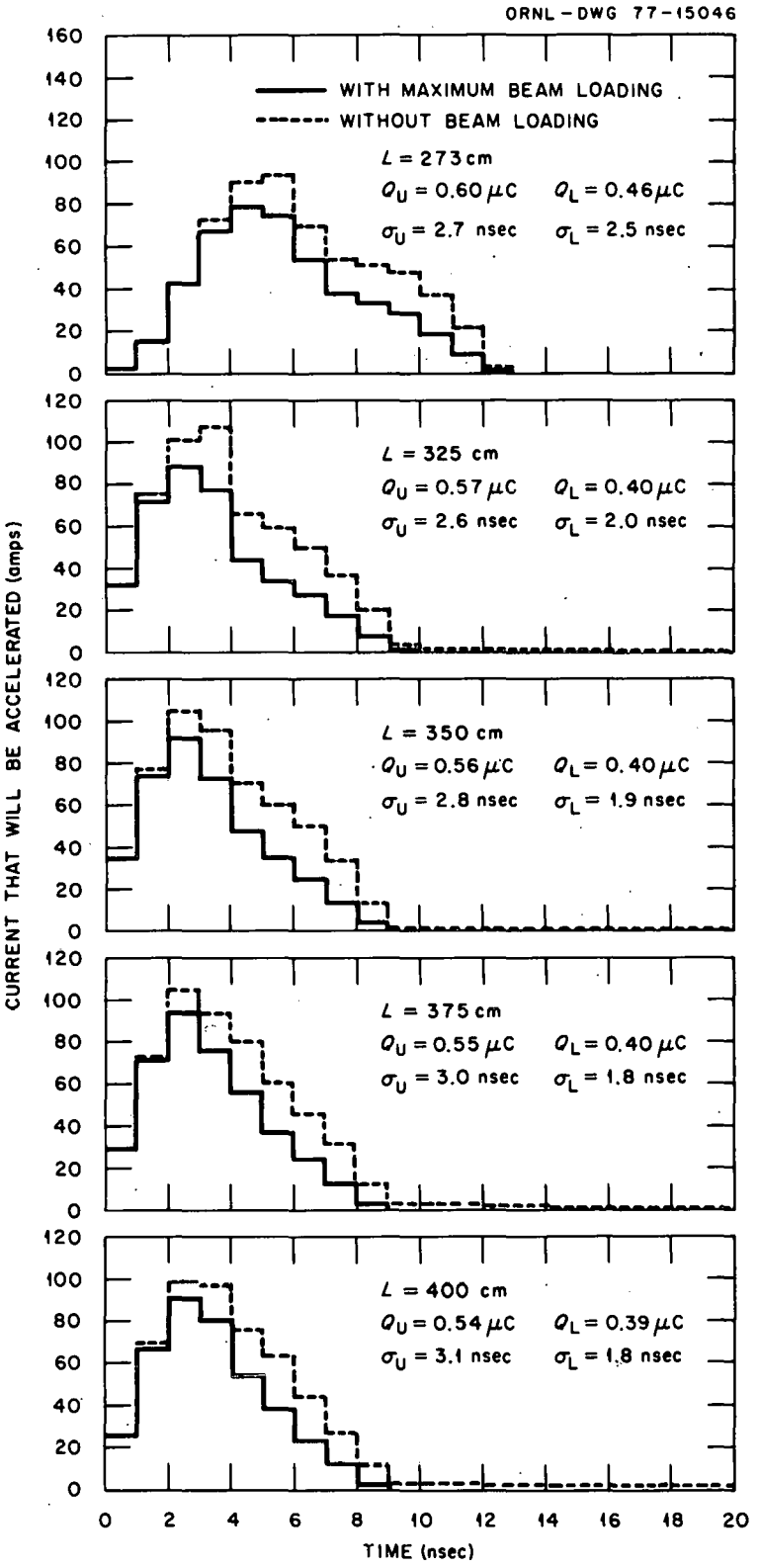

Fig. 5. Current that will be accelerated *vs* time for a 9-voltage gap configuration. (The dashed histogram is the upper bound and the solid histogram is the lower bound.) (Q = 1 μC, r_o = 0.4 cm).

is so small that it cannot be shown on the graph. It is important to note that the tail occurs only on the dashed histogram, i.e., on the upper bound. Since the "tail" occurs on the upper bound as calculated here and not on the lower bound the actual extent to which this tail will occur experimentally is not known from the present calculations. For $L \geqslant 325$ cm the total charge that will be accelerated is slightly smaller in Fig. 5 than in Figs. 3 and 4. If one considers only the solid curves and σ_L in Fig. 5 then the bunching is slightly better than that in Figs. 3 and 4, but because of the effects of the tail the σ_U values in Fig. 5 are appreciably larger than those in Fig. 3 and 4. Since the presence of the tail is undesirable experimentally, it seems that it may be necessary to accept only the bunching provided by the 8 gap configuration in order to avoid a substantial tail.

The results in Figs. 3, 4, and 5 are based on the idealized assumption that the electron beam does not spread radially during its motion. To obtain a very approximate estimate of the effects of radial spreading on the bunching the calculations with the 8-gap configuration have been repeated under the assumption that the beam has a radius of 1.0 cm (rather than 0.4 cm). The results of this calculation are shown in Fig. 6.

The most striking feature of the results in Fig. 6 are the tails on the distribution for $L \geqslant 325$ cm and the fact that the charges that will be accelerated, i.e., Q_U and Q_L, are somewhat lower for $L \geqslant 325$ cm than in the previous figures. Note in particular that at $L = 242$ cm, $Q_U = .61$ μC and $Q_L = .46$ μC while at $L = 325$ cm $Q_U = .44$ μC and $Q_L = .30$ μC. The basic reason for this decrease is the change in the magnetic field that occurs

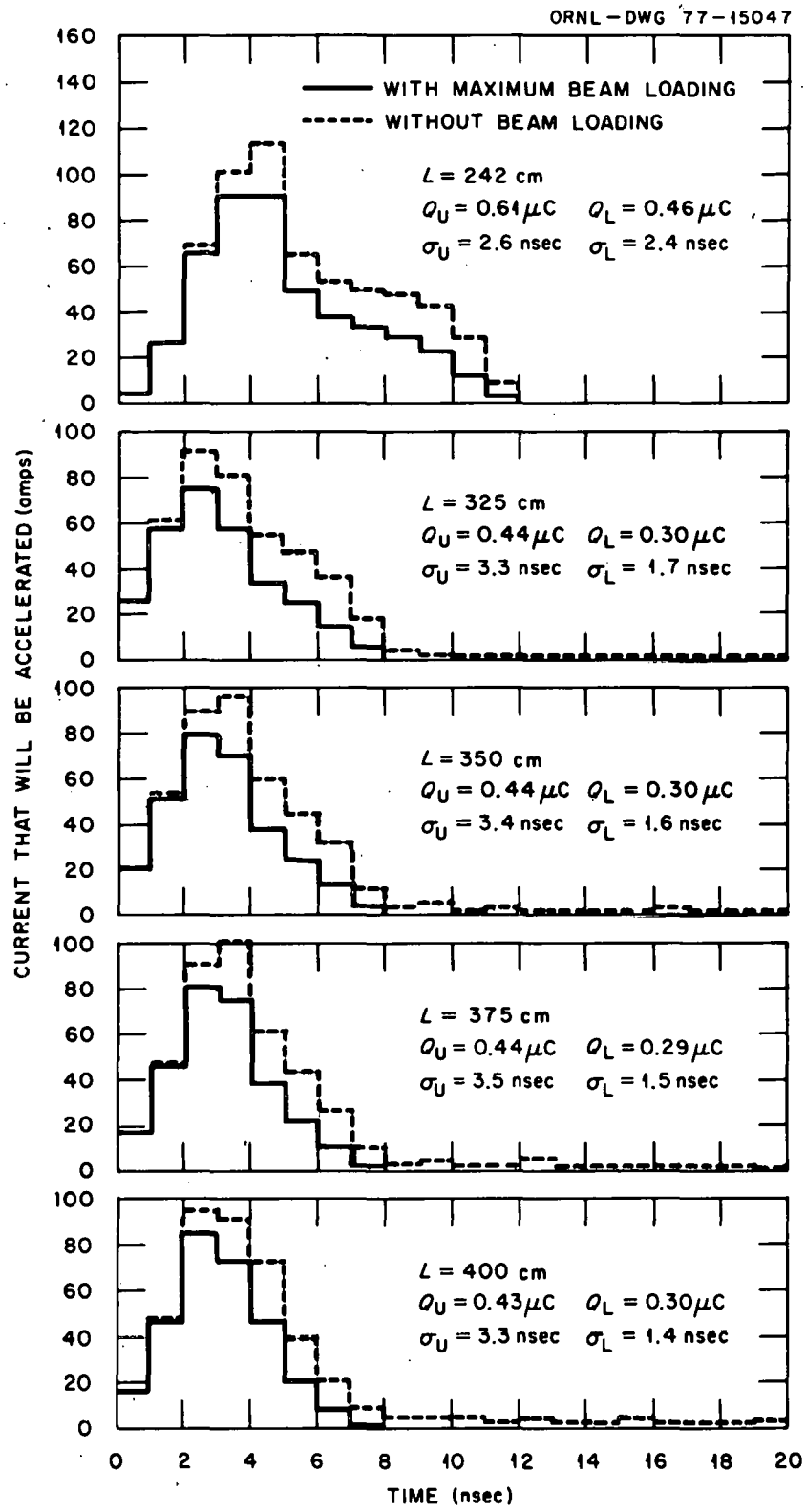

Fig. 6. Current that will be accelerated *vs* time for an 8-voltage gap configuration and a beam radius, r_0, of 1 cm. (The dashed histogram is the upper limit and the solid histogram is the lower limit.) (Q = 1 μC).

between 275 and 300 cm in this case. This inhomogeneous magnetic field acts as a "magnetic mirror" and thereby decreases the longitudinal energy of the particles so that they are less likely to be accelerated when they enter the accelerator. (In some cases the particles attain a negative longitudinal velocity and thereby never reach the accelerator.) This same effect is present in the other cases considered, but it is much smaller when the beam radius is small. The tails on the current distribution calculated without beam loading in Fig. 6 are very similar to those in Fig. 5 and all of the previous discussion concerning these tails applies to those in Fig. 6. The presence of the tails in Fig. 6 indicates that even a configuration that appears to give reasonable bunching (see Fig. 4) may be unsatisfactory from a bunching point of view if there is appreciable radial beam spreading.

SUMMARY

The results of essentially one-dimensional calculations indicate that a 15 nsec (FWHM) electron current pulse can be bunched to approximately 4 nsec (FWHM) by the prebuncher considered here. The bunched beam, however, has a tendency to develop an undesirable "tail", and it may be necessary experimentally to accept a modest amount of bunching in order to avoid a substantial tail.

APPENDIX 1

SPACE CHARGE FIELD

In this appendix the space charge electric field given by Eq. (12) is derived. The derivation presented here is very similar to that of Williams and McGregor[4], but the result is slightly different from that obtained by these authors.

The potential of a point charge at rest inside a conducting cylinder (assumed infinite in length) may be written[7]

$$V' = \frac{2e}{a^2} \sum_{r=1}^{\infty} \sum_{s=0}^{\infty} (2-\delta_s^0) \exp[-\mu_r |z_i' - z_j'|] \frac{J_s(\mu_r b) J_s(\mu_r \rho)}{\mu_r [J_{s+1}(\mu_r a)]^2} \cos s(\phi - \phi_0) \tag{A1.1}$$

where

a = the radius of the conducting cylinder;

z_j', b, ϕ_0 = the polar coordinates of the point charge;

z_i', ρ, ϕ = the polar coordinates of the field point;

J_s = a Bessel function of the first kind[7],

$$\delta_s^0 = 1 \quad \text{if } s = 0$$
$$= 0 \quad \text{if } s \neq 0 \tag{A1.2}$$

and μ_r is defined from the zeros of J_0 by the equation

$$J_0(\mu_r a) = 0. \tag{A1.3}$$

The electric field in the z direction is given by

$$E_z' = - \frac{\partial V'}{\partial z_i'} \tag{A1.4}$$

so

$$E'_z = \frac{2e}{a^2} \sum_{r=1}^{\infty} \sum_{s=0}^{\infty} (2-\delta_s^\circ)\exp[-\mu_r|z'_i-z'_j|]\text{sign}(z'_i-z'_j) \cdot \frac{J_s(\mu_r b)J_s(\mu_r \rho)\cos s(\phi-\phi_0)}{(J_{s+1}(\mu_i a)]^2} \tag{A1.5}$$

This is the electric field in the system where the point charge is at rest. If the point charge is moving in the z direction with a velocity $\dot{z}_j$ and if it is assumed that the Lorentz transformation is valid when the conducting cylinder is present then

$$E_z = \frac{2e}{a^2} \sum_{r=1}^{\infty} \sum_{s=0}^{\infty} (2-\delta_s^\circ)\exp[-\mu_r \gamma_{zj}|z_i-z_j|]\text{sign}\,(z_i-z_j) \cdot \frac{J_s(\mu_r b)J_s(\mu_r \rho)\cos s(\phi-\phi_0)}{[J_{s+1}(\mu_r a)]^2} \tag{A1.6}$$

$$\gamma_{zj} = \frac{1}{\sqrt{1-\beta_j^2}} , \tag{A1.7}$$

where

E_z = the electric field in the laboratory system;

z_j, b, ϕ_0 = the polar coordinates of the point charge in the laboratory system;

z_i, ρ, ϕ = the polar coordinates of the field point in the laboratory system.

In obtaining (A1.6) the fact that E_z is invariant under a Lorentz transformation along the z axis and that

$$z'_i - z'_j = \gamma_{zj}(z_i - z_j) \tag{A1.8}$$

have been used.

Equation (A1.6) is the field from a point charge, but to obtain the field E_s that appears in Eq. (A1.5) it is necessary to integrate over the spatial extent of the source "disk" and to average over the spatial extent of the fixed "disk". That is,

$$E_s(z_i, z_j, \beta_j) = \frac{\int_0^{2\pi}\int_0^{r_0}\int_0^{2\pi}\int_0^{r_0} E_z \frac{q_s q_f}{e}\, db d\phi_0 \rho d\rho d\phi}{\int_0^{2\pi}\int_0^{r_0} q_f\, \rho d\rho d\phi} \tag{A1.9}$$

where

q_s = the charge density of the source "disk", and

q_f = the charge density of the field "disk".

Assuming that the charge densities are constant over the "disks" the integrations in Eq. (A1.9) may be carried out in a straightforward manner as shown by Williams and McGregor[4] to give

$$E_s(z_i,z_j,\beta_j) = \frac{2}{r_0^2} \sum_{r=1}^{\infty} \exp\left[-\gamma_r \frac{\gamma_r}{a}|z_i - z_j|\right] \cdot \left[\frac{2J_1\left(\gamma_r \frac{r_0}{a}\right)}{\gamma_r J_1(\gamma_r)}\right]^2 \operatorname{sign}(z_i - z_j) \tag{A1.10}$$

This expression for E_s is still not directly useable in Eq. (A1.5) because Eq. (A1.10) was derived assuming β_j to be constant and the β_j in Eq. (A1.5) is changing with time. It will thus further be assumed that Eq. (A1.10) remains approximately valid when β_j is changing with time, i.e., the Lorentz transformation used in the derivation is assumed to be approximately valid if carried out at the instantaneous value of β_j.

The expression for E_s given in Eq. (A1.10) differs from that used by Williams and McGregor[4] only in that they replace the exponential factor

$$\exp[-\gamma_{zj} \frac{\gamma_r}{a}|z_i - z_j|]$$

by

$$\exp[-\frac{1}{2}(\gamma_{zi}+\gamma_{zj})\frac{\gamma_r}{a}|z_i - z_j|].$$

Both forms are, of course, very approximate.

APPENDIX 2

BEAM LOADING

In this appendix the beam-loading results introduced in Section 2.4 are derived. The derivation given below is taken from the work of Neal[9] and Leiss.[10]

The equation governing the flow of rf power in the accelerator may be written[9]

$$\frac{dP(z_A,t)}{dz_A} = - 2I_A(z_A)\, P(z_A,t) - i(z_A,t)\, E_A(z_A,t) \quad , \tag{A2.1}$$

where

$P(z_A,t)$ = the power at point z_A at time t,

$I_A(z_A)$ = the voltage attenuation coefficient at z_A,

$i(z_A,t)$ = the electron current at z_A and t,

$E_A(z_A,t)$ = the electric field amplitude at z_At,

and where the approximation has been made that the electrons travel on the crest of the wave from the time they enter the accelerator and are not lost to the walls. These approximations are not valid near the beginning of the accelerator, and thus the derivation presented here is not applicable for small values of z_A. Using the expression for the shunt impedance, r, of the wave guide,[10]

$$P(z_A,t) = \frac{E_A^2(z_A,t)}{2I_A(z_A)r} \quad , \tag{A2.2}$$

and the expression for $I_A(z)$ derived by Neal[9] for an accelerator of the ORELA type,

$$I_A(z_A) = \frac{\gamma_A}{2(P_1 - \gamma_A z_A)} \tag{A2.3}$$

where

γ_A = the average power expenditure per unit length in the accelerator (= constant),

P_1 = the input rf power,

Eq. (A2.1) may be rewritten as

$$\frac{\partial E(z_A,t)}{\partial t} + v_g \frac{\partial E(z_A,t)}{\partial z} = -v_g I_A(z_A)\, r\, i(z_A,t) \quad , \tag{A2.4}$$

where

v_g = the group velocity in the wave guide.

To solve Eq.(A2.4), the Laplace transform with respect to time is taken to give

$$\frac{\partial E(z_A,s)}{\partial z_A} + \frac{s}{v_g} E(z_A,s) = \frac{1}{v_g} E(z_A,0) - r\, I_A(z_A)\, i(z_A,s) \; . \tag{A2.5}$$

The general solution to Eq. (A2.5) may be written

$$E_A(z_A,s) = E_A(0,s) \exp\left(-\frac{s}{v_g} z_A\right)$$

$$- r \int_0^{z_A} dz'_A I_A(z'_A) \exp\left[-\frac{s}{v_g}(z_A - z'_A)\right] i(z'_A,s)$$

$$+ \int_0^{z_A} dz'_A \frac{E(z'_A,0)}{v_g} \exp\left[-\frac{s}{v_g}(z_A - z'_A)\right] , \tag{A2.6}$$

and inverting the transforms

$$E_A(z_A,t) = E_A\left(0,t - \frac{z_A}{v_g}\right) \Theta\left(t - \frac{z_A}{v_g}\right)$$

$$+ \int_0^{z_A} dz'_A \frac{E_A(z'_A,0)}{v_g} \delta\left(t - \frac{z_A - z'_A}{v_g}\right)$$

$$- r \int_0^{z_A} dz'_A I_A(z'_A)\, i\left(z_A, t - \frac{z_A - z'_A}{v_g}\right) \Theta\left(t - \frac{z_A - z'_A}{v_g}\right) \qquad \text{(A2.7)}$$

$$E_A(z_A,t) = E_A\left(0,t - \frac{z_A}{v_g}\right) \Theta\left(t - \frac{z_A}{v_g}\right)$$

$$+ E_A(z_A - v_g\, t,0)\, \Theta(z_A - v_g\, t)$$

$$- r \int_0^{z_A} dz'_A\, I(z'_A)\, i\left(z'_A, t - \frac{z_A - z'_A}{v_g}\right) \Theta\left(t - \frac{z_A - z'_A}{v_g}\right) \quad . \qquad \text{(A2.8)}$$

For boundary conditions, it will be assumed that

$$E_A(z_A,0) = E_{A0}$$

$$E_A(0,t) = E_{A0} \quad ,$$

where E_{A0} = constant, so Eq. (A2.8) becomes

$$E_A(z_A,t) = E_{A0} - r \int_{(z_A - v_g t)\,\Theta(z_A - v_g t)}^{z_A} dz'_A I_A(z'_A)\, i\left(z'_A, t - \frac{z_A - z'_A}{v_g}\right) , \qquad \text{(A2.9)}$$

where the lower limit has been determined from the Θ function in Eq. (A2.9) To proceed further, the current, $i(z_A,t)$, will be specified to be

$$i(z_A,t) = i_A\, \Theta\left(t - t_{A10} - \frac{z_A}{c}\right) \quad , \qquad \text{(A2.10)}$$

where

i_A = constant,

t_{A10} = the time when first electron enters the accelerator,

c = the particle velocity in the accelerator which is assumed to be constant and equal to the velocity of light,

that is, the current in the accelerator will be assumed to be a constant except that it is turned on at $t = t_{A10}$. If Eq. (A2.10) is substituted in Eq. (A2.9), and T is defined by

$$T = t - t_{A10} - \frac{z_A}{v_g} + z'_A\left(\frac{1}{v_g} - \frac{1}{c}\right)$$

one finds

$$E_A(z,t) = E_{A0} - \frac{ri_A}{\left(\frac{1}{v_g} - \frac{1}{c}\right)} \int_{(t-t_{A10}-\frac{z_A}{v_g})\Theta(t-t_{A10}-\frac{z_A}{v_g})}^{t-t_{A10}-\frac{z_A}{c}} I_A[z'_A(T)]dT \quad , \qquad \text{(A2.11)}$$

$$I_A[z'_A(T)] = \frac{\gamma_A}{2[P_1 - \gamma_A z'_A(T)]} \qquad \text{(A2.12)}$$

Equations (A2.11) and (A2.12) may be used to obtain an exact expression for $E_A(z,t)$, but for our purposes it will be convenient to proceed in a much more approximate manner. First, note that current pulses of only $\sim$ 15 nsec duration are of interest and $v_g = 0.007\ c$,[1,2] so the lower limit on the integral in Eq. (A2.11) is different from zero during the pulse only for $z_a \leqslant 3$ to 4 cm. Since Eq. (A2.11) is not valid in any case at small z_A

because of the constant current assumption, the lower limit may be taken to be zero with the understanding that small values of z_A are not to be considered. Then, using the mean-value theorem, for sufficiently large z_A Eq. (A2.11) becomes

$$E_A(z_A,t) = E_{A0} - r\,\bar{I}_A v_g i_A[t-t_{A10} - \frac{z_A}{c}] \quad , \tag{A2.13}$$

where

$\bar{I}_A$ = some mean value of I_A that is to be specified.

Now let us evaluate Eq. (A2.13) at the position of the $i^{\underline{th}}$ electron as it moves in the accelerator. Since

$$z_{Ai} = c\,(t - t_{Ai0}) \quad , \tag{A2.14}$$

where

t_{Ai} = the time when the $i^{\underline{th}}$ electron enters the accelerator,

one finds

$$E_A(z_{Ai},t) = E_{A0} - r\,\bar{I}_A v_g i_A[t_{Ai0} - t_{Ai0}] \tag{A2.15}$$

$$= E_{A0} - r\,\bar{I}_A v_g Q_{Ai} \tag{A2.16}$$

$$Q_{Ai} = i_A[t_{Ai0} - t_{A10}] \quad , \tag{A2.17}$$

where

Q_{Ai} = the charge that is being accelerated in front of the ith electron.

Equation (A2.16) indicates that the electric field amplitude at the position of the $i^{\underline{th}}$ electron as it moves in the accelerator is approximately a constant independent of time.

To determine the constant in Eq. (A2.16), the energy change of the electrons at small z_A, is neglected as it is negligible compared with the energy of the electrons at the end of the accelerator, and thus the energy spread of the electron pulse, $\Delta\varepsilon$, as it leaves the accelerator is given approximately by

$$\Delta\varepsilon = e\, r\, \bar{I}_A v_g Q_A L_A \qquad \text{(A2.18)}$$

where

Q_A = the total charge that is accelerated, and

L_A = the length of the accelerator.

Measurements of the energy spread of the current pulse as a function of accelerated charge have been made at ORELA, and the linear relationship given in Eq.(A2.18) has been shown to be quite valid.[1,2] Furthermore, from the measurements the constant in Eq.(A2.18) can be obtained and is found to be

$$K = r\bar{I}_A v_g$$

$$= \frac{7.3\ \text{MV}}{\mu\text{C m}}$$

It is this empirical value that was used in obtaining the results presented in Section 3. The manner in which the beam-loading results are used is discussed in Section 2.4.

REFERENCES

1. N. C. Pering and T. A. Lewis, "Performance of 140 MeV High Current Short Pulse Linac at ORNL," IEEE Trans. on Nucl. Sci., NS-16 (3), 316 (1969).
2. T. A. Lewis, "ORELA Performance," ORNL/TM-5112, Oak Ridge National Laboratory (1976).
3. P. Tien, L. Walker, and V. Wolontes, "A Large Signal Theory of Traveling-Wave Amplifiers," Proc. IRE, Vol. 43, March 1955, pp. 260-277.
4. C. B. Williams and M. H. MacGregor, "Space Charge Effects in High Current Linear Electron Accelerator Injection Systems," IEEE Trans. Nucl. Sci., NS-14 (3), (1967).
5. P. J. Tallerico, "Large-Signal Effects in the Multicavity Klystron," LA 4389, UC-34 Physics, TID-4500 (1970).
6. J. E. Rowe, Non-Linear Electron Wave Interaction Phenomena, Academic Press, New York, 1965.
7. W. R. Smythe, Static and Dynamic Electricity, McGraw-Hill Book Co., Inc., New York, NY (Third Edition) (1968).
8. J. C. Slater, Microwave Electronics, D. Van Nostrand Co., New York, Chapter XI, (1950).
9. R. B. Neal, "Theory of the Constant Gradient Linear Electron Accelerator," Microwave Laboratory Report No. 513, W. W. Hansen Laboratory of Physics, Stanford University, Stanford, CA (1958).
10. J. E. Leiss, "Transient Beam Loading in Linear Electron Accelerators," National Bureau of Standards Internal Memo, September 29, 1958.

THIS PAGE

WAS INTENTIONALLY

LEFT BLANK

ORNL/TM-5419

INTERNAL DISTRIBUTION

1-3. L. S. Abbott
4-8. F. S. Alsmiller
9-30. R. G. Alsmiller, Jr.
31-35. J. Barish
36. D. W. Bible
37. C. J. Borkowski
38. G. T. Chapman
39. J. W. T. Dabbs
40. G. De Saussure
41. R. L. Ferguson
42. J. L. Fowler
43. C. Y. Fue
44. T. A. Gabriel
45. H. Goldstein (consultant)
46. R. Gwin
47. J. Halperin
48. J. A. Harvey
49. N. W. Hill
50. R. W. Ingle
51. C. H. Johnson
52. D. C. Larson
53. T. A. Lewis
54. R. A. Lillie
55. R. L. Macklin
56. F. C. Maienschein
57. F. W. Manning
58. B. F. Maskewitz
59. J. W. McConnell
60. J. T. Mihalczo
61. H. A. Mook
62. R. M. Moon
63. G. L. Morgan
64. D. K. Olsen
65. R. W. Peelle
66. F. G. Perey
67. R. B. Perez
68. S. Raman
69. R. T. Santoro
70. G. G. Slaughter
71. R. R. Spencer
72. P. H. Stelson
73. M. L. Tobias
74. H. A. Todd
75. J. H. Todd
76. L. W. Weston
77. A. Zucker
78. P. Greebler (consultant)
79. W. W. Havens, Jr. (consultant)
80. A. F. Henry (consultant)
81. R. E. Uhrig (consultant)
82-83. Central Research Library
84. ORNL Y-12 Technical Library Document Reference Section
85-86. Laboratory Records Department
87. Laboratory Records ORNL RC
88. ORNL Patent Office

EXTERNAL DISTRIBUTION

89. USERDA Oak Ridge Operations, Research and Technical Support Division, P. O. Box E, Oak Ridge, TN 37830: Director
90. E. T. Ritter, Division of Physical Research, U.S. Energy Research and Development Administration, Washington, DC 20545
91. G. L. Rogosa, Asst. Dir. for Nuclear Sciences, Division of Physical Research, U.S. Energy Research and Development Administration, Washington, DC 20545
92. S. L. Whetstone, Division of Physical Research, U.S. Energy Research and Development Administration, Washington, DC 20545
93. P. B. Hemmig, Chief, Physics Branch, Div. of Reactor Development and Demonstration, U.S. Energy Research and Development Administration, Washington, DC 20545
94-95. C. D. Bowman and J. E. Lease, National Bureau of Standards, Center for Radiation Research, Nuclear Radiation Division, Washington, DC 20234

96. M. S. Moore, Los Alamos Scientific Laboratory, P.O. Box 1663, Los Alamos, NM 87544
97. R. C. Block, Rensselaer Polytechnic Institute, Troy, NY 12181
98. N. C. Pering, 611 Hansen Way, Palo Alto, CA 94303
99. R. R. Winter, Denison University, Granville, OH 43023
100-126. Technical Information Center (TIC)